Monthly Notices
of the
ROYAL ASTRONOMICAL SOCIETY

MNRAS **441,** 3703–3717 (2014) doi:10.1093/mnras/stu824

Dynamics of stellar black holes in young star clusters with different metallicities – II. Black hole–black hole binaries

Brunetto Marco Ziosi,[1,2]★ Michela Mapelli,[2] Marica Branchesi[3,4,5] and Giuseppe Tormen[1]

[1] *Università degli Studi di Padova, Vicolo dell'Osservatorio 3, I-35122, Padova, Italy*
[2] *INAF – Osservatorio Astronomico di Padova, Vicolo dell'Osservatorio 5, I-35122, Padova, Italy*
[3] *Università degli Studi di Urbino 'Carlo Bo', Dipartimento di Scienze di Base e Fondamenti, Piazza della Repubblica 13, I-61029, Urbino, Italy*
[4] *INAF – Osservatorio Astronomico di Roma, Via Frascati 33, I-00040, Monte Porzio Catone (RM), Italy*
[5] *INFN, Sezione di Firenze, I-50019 Sesto Fiorentino, Firenze, Italy*

Accepted 2014 April 24. Received 2014 April 19; in original form 2014 February 28

ABSTRACT

In this paper, we study the formation and dynamical evolution of black hole–black hole (BH–BH) binaries in young star clusters (YSCs), by means of *N*-body simulations. The simulations include metallicity-dependent recipes for stellar evolution and stellar winds, and have been run for three different metallicities ($Z = 0.01, 0.1$ and $1\ Z_{\odot}$). Following recent theoretical models of wind mass-loss and core-collapse supernovae, we assume that the mass of the stellar remnants depends on the metallicity of the progenitor stars. We find that BH–BH binaries form efficiently because of dynamical exchanges: in our simulations, we find about 10 times more BH–BH binaries than double neutron star binaries. The simulated BH–BH binaries form earlier in metal-poor YSCs, which host more massive black holes (BHs) than in metal-rich YSCs. The simulated BH–BH binaries have very large chirp masses (up to $80\ M_{\odot}$), because the BH mass is assumed to depend on metallicity, and because BHs can grow in mass due to the merger with stars. The simulated BH–BH binaries span a wide range of orbital periods (10^{-3}–10^{7} yr), and only a small fraction of them (0.3 per cent) is expected to merge within a Hubble time. We discuss the estimated merger rate from our simulations and the implications for Advanced VIRGO and LIGO.

Key words: black hole physics – gravitational waves – methods: numerical – binaries: general – galaxies: star clusters: general.

1 INTRODUCTION

Most stars are expected to form in young star clusters (YSCs; Carpenter 2000; Lada & Lada 2003; Porras et al. 2003). Like globular clusters (GCs), the densest YSCs are collisional systems: their two-body relaxation time-scale is shorter than their lifetime, and they undergo intense dynamical evolution. On the other hand, YSCs are considerably different from GCs: the former have generally lower mass ($<10^5\ M_{\odot}$) and smaller size (half-mass radius $r_{\rm hm} \lesssim 1$ pc) than the latter (see e.g. Portegies Zwart, McMillan & Gieles 2010, for a recent review). This explains why the central relaxation time of YSCs is ∼10–50 Myr orders of magnitude shorter than that of GCs (e.g. Portegies Zwart 2004). YSCs populate the disc of late-type galaxies, while GCs are spherically distributed in the host-galaxy halo. Finally, GCs are old ($\gtrsim$12 Gyr) and long-lived systems, whereas YSCs are young and short lived: most of them dissolve in the disc of the host galaxy in $\leq 10^8$ yr (e.g. Kruijssen et al. 2011).

Thus, the stellar content of dissolved YSCs is expected to build up a considerable fraction of the field population of the host galaxy. This must be taken into account when modelling the evolution of binary stellar systems in the galactic field: a large fraction of these binaries likely formed in YSCs, and then evolved through intense dynamical interactions, before being ejected into the field after the disruption of the parent YSC. This scenario is important for the study of stellar black hole (BH) binaries. In Mapelli et al. (2013, hereafter Paper I), we studied the formation and the dynamical evolution of accreting BH binaries in YSCs. We found that dynamical interactions in YSCs have a significant impact on the expected population of X-ray sources powered by BHs.

In the current paper, we study the formation and the dynamical evolution of black hole–black hole (BH–BH) binaries in YSCs. For the sake of completeness, we will compare the evolution of BH–BH binaries with that of neutron star–neutron star (NS–NS) binaries and with that of binaries composed of a BH and a

★ E-mail: brunetto.ziosi@gmail.com

neutron star (NS) in YSCs. BH–BH, NS–NS and NS–BH binaries are among the most promising sources of gravitational waves (GWs) detectable by ground-based detectors (e.g. Peters 1964; Abramovici et al. 1992). Understanding the demographics of such double compact object binaries (DCOBs) is particularly important in light of the forthcoming second-generation ground-based GW detectors, Advanced LIGO and VIRGO (Acernese et al. 2009; Harry 2010; Accadia et al. 2012).

The dynamics of YSCs can influence the formation and evolution of BH–BH binaries in three different ways: (i) dynamical friction causes the BHs (which are more massive than most stars) to sink to the denser YSC core, where they have a higher probability to interact with other BHs (e.g. Sigurdsson & Hernquist 1993); (ii) three-body encounters (i.e. close encounters between a binary and a single star) change the binary orbital properties: if the binary is hard (i.e. if its binding energy is higher than the average kinetic energy of a star in the cluster[1]), three-body encounters tend to shrink the binary semi-major axis (Heggie 1975); (iii) dynamical exchanges (i.e. three-body interactions in which one of the members of the binary is replaced by the single star) enhance the formation of BH–BH binaries. In fact, the probability for a single star with mass m_3 to replace a binary member is higher if $m_3 \geq m_1$ or $m_3 \geq m_2$ (where m_1 and m_2 are the masses of the former binary members; see Hills 1989, 1992). As BHs are more massive than most stars, they efficiently acquire companions through dynamical exchanges.

Previous studies investigated the formation and evolution of DCOBs either in GCs, via Monte Carlo codes (e.g. O'Leary et al. 2006; Sadowski et al. 2008; Downing et al. 2010, 2011; Clausen, Sigurdsson & Chernoff 2013), or in the field, using population synthesis simulations of isolated binaries (e.g. Belczynski, Kalogera & Bulik 2002; Voss & Tauris 2003; Pfahl, Podsiadlowski & Rappaport 2005; Dewi, Podsiadlowski & Sena 2006; Belczynski et al. 2007, 2010a; Dominik et al. 2012). Our study provides a new perspective on this subject: we study the formation of BH–BH binaries in YSCs, by using direct *N*-body simulations coupled with up-to-date stellar and binary evolution recipes. The paper is organized as follows. In Section 2, we briefly describe our simulations. In Section 3, we present our results. Section 4 is devoted to discuss the results and to compare them with previous work. Our conclusions are presented in Section 5.

2 METHODS AND SIMULATIONS

The simulations analysed in this paper adopt the same technique as described in Paper I. In particular, we used a modified version of the STARLAB public software environment (see Portegies Zwart et al. 2001). Our upgraded version of STARLAB includes (i) analytic formulae for stellar evolution as a function of mass and metallicity (Hurley, Pols & Tout 2000), (ii) metallicity-dependent stellar winds for main sequence (Vink, de Koter & Lamers 2001) and evolved stars (Vink & de Koeter 2005) and (iii) the possibility that massive BHs form by direct collapse, i.e. with a weak or no supernova (SN) explosion (e.g. Fryer 1999; Fryer & Kalogera 2001; Mapelli, Colpi & Zampieri 2009; Belczynski et al. 2010b; Fryer et al. 2012).

According to these recipes, if the final mass of the progenitor star (i.e. the mass before the collapse), is $>40\ \mathrm{M}_\odot$, we assume that the SN fails and that the star collapses quietly to a BH. As the final mass of a massive star is higher at low metallicity, because of the weaker stellar winds, BH masses are allowed to be higher at low metallicity. In particular, the BH mass depends on the metallicity and on the zero-age main-sequence mass of the progenitor as described in fig. 1 of Paper I. In this scenario, BHs with mass up to $\sim 80\ \mathrm{M}_\odot$ ($\sim 40\ \mathrm{M}_\odot$) can form if the metallicity of the progenitor is $Z \sim 0.01\ \mathrm{Z}_\odot$ ($Z \sim 0.1\ \mathrm{Z}_\odot$). The maximum BH mass at $Z \sim \mathrm{Z}_\odot$ is $23\ \mathrm{M}_\odot$. This is higher than that assumed in previous studies (e.g. Belczynski et al. 2010b), but is still consistent with the observations, given the large uncertainties (e.g. Özel et al. 2010).

NSs and BHs that form from an SN explosion receive a natal kick in a random direction. The natal kick of NSs is chosen randomly from the distribution $P(u) = (4/\pi)\,(1+u^2)^{-2}$, where $u = v/\tilde{v}$, v is the modulus of the velocity vector of the NS and $\tilde{v} = 600\ \mathrm{km\ s^{-1}}$ (Hartman 1997; Portegies Zwart et al. 2001). The natal kick of BHs is drawn from the same distribution, but is normalized by a factor $f_{\rm kick} = (m_{\rm NS}/m_{\rm BH})^{1/2}$ (where $m_{\rm BH}$ is the BH mass and $m_{\rm NS} = 1.3\ \mathrm{M}_\odot$ is the typical NS mass). Instead, BHs that form from quiet collapse are assumed to receive no natal kick (see Fryer et al. 2012).

Furthermore, STARLAB includes recipes for binary evolution, such as mass transfer (via wind accretion and via Roche lobe overflow), tidal circularization, magnetic braking and also orbital decay and circularization by GW emission (see Portegies Zwart & Verbunt 1996; Portegies Zwart et al. 2001).

We doubled the simulation sample with respect to Paper I: we have 600 *N*-body realizations of YSCs (1/3 of them with solar metallicity, 1/3 with metallicity $Z = 0.1\ \mathrm{Z}_\odot$ and the remaining 1/3 with $Z = 0.01\ \mathrm{Z}_\odot$). Half of the simulations were already presented in Paper I, whereas the remaining are new simulations.

The simulated YSCs are initially modelled with 5000 centres of mass (single stars or binaries), following a King profile with central dimensionless potential $W_0 = 5$. The core density at the beginning of the simulation is $\rho_{\rm C} \sim 2 \times 10^3\ \mathrm{M}_\odot\ \mathrm{pc}^{-3}$. We chose a primordial binary fraction of $f_{\rm PB} = 0.1$ so the total number of stars is $N_* = 5500$. The total mass of a single YSC is $M_{\rm TOT} \sim 3{-}4 \times 10^3\ \mathrm{M}_\odot$. The single stars and the primary stars (m_1) of the binaries follow a Kroupa initial mass function (IMF; Kroupa 2001) with minimum and maximum mass equal to 0.1 and $150\ \mathrm{M}_\odot$, respectively. The masses of the secondaries (m_2) are generated according to a uniform distribution between $0.1m_1$ and m_1. The initial semi-major axis a of the binaries are drawn from a log-uniform distribution $f(a) \propto 1/a$ between $\mathrm{R}_\odot$ and $10^5\ \mathrm{R}_\odot$, for consistency with the observation of binaries in the solar neighbourhood (Kraicheva et al. 1978; Duquennoy & Mayor 1991). Values of a leading to a periastron separation smaller than the sum of the radii of the two stars in the binary were discarded. We randomly select the initial eccentricity from a thermal distribution $f(e) = 2\,e$ in the range [0, 1] (Heggie 1975).

The central relaxation time-scale is (Portegies Zwart 2004) $t_{\rm rlx} \sim 10\ \mathrm{Myr}\,(r_{\rm hm}/0.8\ \mathrm{pc})^{3/2}(M_{\rm TOT}/3500\ \mathrm{M}_\odot)^{1/2}$, where $r_{\rm hm}$ is the half-mass radius of the YSC ($\sim 0.8{-}0.9$ pc in our simulations). The core-collapse time-scale (Portegies Zwart & McMillan 2002) is $t_{\rm cc} \sim 2\,\mathrm{Myr}(t_{\rm rlx}/10\ \mathrm{Myr})$.

A summary of the properties of the simulated YSCs is shown in Table 1. These were chosen to match the properties of the most common YSCs in our Galaxy.

[1] A binary can be classified as hard if its binding energy is higher than the average kinetic energy of stars in the cluster, that is,

$$\frac{G\,m_1\,m_2}{2\,a} \gtrsim \frac{1}{2}\langle m\rangle\sigma^2, \quad (1)$$

where G is the gravitational constant, m_1 and m_2 are the mass of the primary member and the mass of the secondary member of the binary, respectively, while $\langle m\rangle$ and σ are the average mass and velocity dispersion of a star in the star cluster.

Table 1. Summary of initial YSC properties. W_0: central dimensionless potential in the King (1966) model; N_*: number of stars per YSC; r_c: initial core radius; $c \equiv \log_{10}(r_t/r_c)$: concentration ($r_t$ is the initial tidal radius); IMF: initial mass function; m_{min} and m_{max}: minimum and maximum simulated stellar mass, respectively; Z: metallicity of the YSC (in our simulations, we assume $Z_\odot = 0.019$); t_{max}: duration of each simulation (in Myr); f_{PB}: fraction of PBs, defined as the number of PBs in each YSC divided by the number of 'centres of mass' (CMs) in the YSC. In each simulated YSC, there are initially 5000 CMs, among which 500 are designated as 'binaries' and 4500 are 'single stars' (see Downing et al. 2010 for a description of this formalism). Thus, 1000 stars per YSC are initially in binaries.

Parameter	Value
W_0	5
N_*	5500
r_c (pc)	0.4
$c \equiv \log_{10}(r_t/r_c)$	1.03
IMF	Kroupa (2001)
m_{min} ($M_\odot$)	0.1
m_{max} ($M_\odot$)	150
Z ($Z_\odot$)	0.01, 0.1, 1
t_{max} (Myr)	100
f_{PB}	0.1

Each YSC was simulated for 100 Myr: at later times, the YSCs are expected to be disrupted by the galactic tidal field (e.g. Goddard, Bastian & Kennicutt 2010; Silva-Villa & Larsen 2010; Gieles & Portegies Zwart 2011). We do not use recipes for the galactic tidal field but they will be included in future work. The structural evolution of our simulated YSCs is described in a companion paper (Mapelli & Bressan 2013). From fig. 4 of Mapelli & Bressan (2013), it is apparent that the half-mass radius of the YSCs at 100 Myr is ∼3 times the initial value. The average fraction of stars that are still bound to the YSC at 100 Myr is 0.85−0.9. Thus, the simulated YSCs are expanding but most of them have not evaporated by the end of the simulation. This means that our results likely overestimate the number of dynamical exchanges and three-body encounters in the late stages of YSC life. We do not expect that this severely affects our predictions for the merger rate of BH–BH binaries, since the most intense dynamical activity of the YSCs occurs during (and immediately after) the core collapse (i.e. at $t \gtrsim 3$ Myr), because of the dramatic increase in the core density (by a factor of ≥10). In fact, most of the BH–BH binaries form in the first ∼3–40 Myr (see the discussion in Section 3.1), and the BH–BH systems that are expected to merge in less than a Hubble time (and that are not disrupted before the end of the simulation, see Section 3.5) form at 4−7 Myr. In a forthcoming paper, we will add different models for the galactic tidal field, and we will be able to quantify their impact on the BH–BH binary population.

3 RESULTS

3.1 DCOB population

The number of DCOBs formed in our simulations is summarized in Fig. 1. Here and in the following, unless otherwise specified, a binary is defined as a simulated bound pair (either existing in the initial conditions or formed during the evolution of the YSC, either hard or soft, either stable or unstable depending on the criterion adopted by

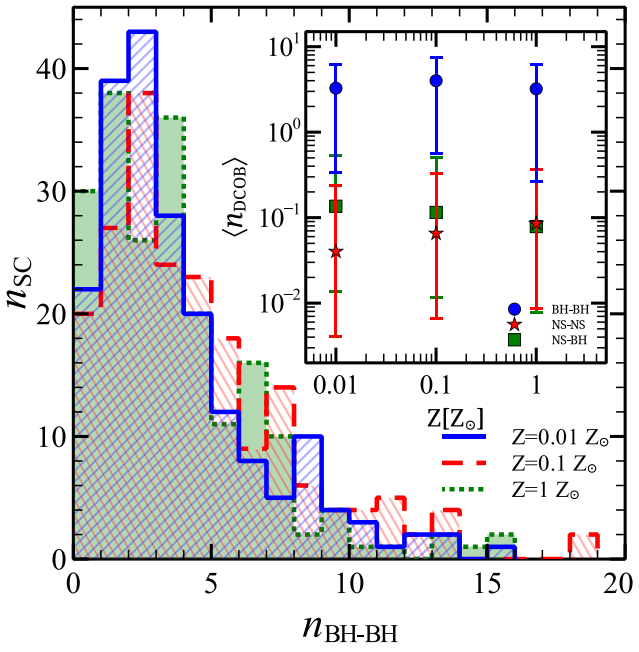

Figure 1. In the main panel, distribution of the number of BH–BH binaries per YSC per metallicity. The blue diagonally hatched histogram refers to $Z = 0.01\,Z_\odot$, the red diagonally hatched histogram to $Z = 0.1\,Z_\odot$ and the green filled histogram to $Z = Z_\odot$. In the inset, average number of BH–BH binaries (blue circles), NS–BH binaries (green squares) and NS–NS binaries (red stars) per YSC as a function of the YSC metallicity. The error bars are 1σ deviations. All the quantities in this figure are integrated over the duration of the simulations (i.e. 100 Myr).

STARLAB; see Portegies Zwart et al. 2001). In Appendix A, we discuss how our main results depend on this definition, by considering stable and unstable binaries separately. Furthermore, we classify a binary that forms from an exchange as a new binary with respect to the pre-exchange binary.

The inset of Fig. 1 shows that the simulated number of BH–BH binaries per YSC (integrated over 100 Myr) is a factor of ∼10–100 higher than the simulated number of NS–NS binaries per YSC, regardless of the metallicity.

Due to the chosen IMF, our simulated YSCs host a number of NSs that is 3−4 times higher than the number of BHs. Thus, the fact that BH–BH binaries are much more numerous than NS–NS binaries is a striking effect of dynamics. BHs are heavier and tend to sink to the centre of the YSC on a time-scale $t_{seg} \sim t_{rlx} \frac{\langle m \rangle}{M_{BH}}$ (O'Leary et al. 2006). Thus, a 40 $M_\odot$ BH sinks towards the centre in ∼0.25 Myr. Once in the dense YSC centre, BHs have a higher probability to interact with other BHs, forming BH–BH binaries. Furthermore, BHs are more massive than most stars in the simulation already at $t \sim 8$ Myr (when the turn-off mass is ∼20 $M_\odot$). Thus, they are particularly efficient in acquiring companions through dynamical exchanges (Hills 1989, 1992). In fact, most of our BH–BH binaries come from dynamical exchanges. Only ∼1.7 per cent of BH–BH binaries come from primordial binaries. Moreover, BHs have a weaker (if any) natal kick with respect to that of NSs. Therefore, they are more likely to remain in the denser regions of the YSC, rather than being ejected.

In contrast, a large fraction of NSs (up to 90 per cent at $t = 100$ Myr) is ejected from the parent YSC as a consequence of natal kicks or dynamical recoil. The few NSs that remain in the YSCs are much lighter than BHs, and thus the probability that they

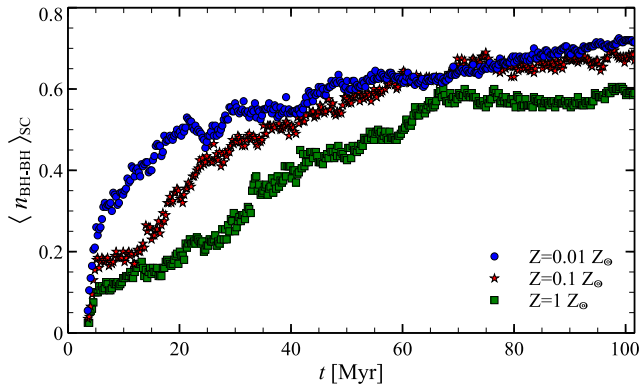

Figure 2. Average number of BH–BH binaries as a function of time for the three different metallicities. Blue circles: $Z = 0.01\,Z_{\odot}$; red stars: $Z = 0.1\,Z_{\odot}$; green squares $Z = 1\,Z_{\odot}$.

acquire a second NS companion by dynamical exchanges is low. This is confirmed by the fact that 87 per cent of all the NS–NS binaries come from primordial binaries.

The main panel of Fig. 1 shows the distribution of the number of BH–BH binaries per YSC per metallicity, integrated over the simulation time ($t_{\rm max} = 100$ Myr). It follows a Poissonian distribution and peaks between two and four BH–BH binaries per YSC, in agreement with the average values shown in the inset of the same figure. Approximately 10−15 per cent of YSCs do not host any BH–BH binary. The simulated YSC with the largest number of BH–BH binaries hosts 18 BH–BH binaries.

We find no statistically significant differences between YSCs with different metallicity, when looking at the number of BH–BH binaries integrated over time (Fig. 1). In contrast, we do find differences when we look at the number of BH–BH binaries as a function of time. In particular, the lower the metallicity is, the shorter the time needed to build the distribution of BH–BH binaries (Fig. 2).

Furthermore, while in the inset of Fig. 1, the average number of BH–BH binaries per YSC (integrated over time) at $Z = 0.1\,Z_{\odot}$ is slightly larger than that at $Z = 0.01\,Z_{\odot}$, in Fig. 2, the number of BH–BH binaries as a function of time at $Z = 0.01\,Z_{\odot}$ is always higher than that at $Z = 0.1\,Z_{\odot}$. This result might appear puzzling: the number of BH–BH binaries per YSC integrated over time is larger at $Z = 0.1\,Z_{\odot}$ than at $Z = 0.01\,Z_{\odot}$, while the number of BH–BH binaries per YSC at a given time is larger at $Z = 0.01\,Z_{\odot}$ than at $Z = 0.1\,Z_{\odot}$. Actually, this is a consequence of the fact that BHs are more massive at low metallicity, and thus are more efficient in acquiring companions through dynamical exchanges and in producing stable binaries with longer lifetimes. This implies that the BH–BH binaries which form at $Z = 0.01\,Z_{\odot}$ are less numerous than those which form at $Z = 0.1$and $1\,Z_{\odot}$ but they live for a much longer time (before being ionized or exchanged) than the latter (see Fig. 3 and the comments in next section). Thus, if we look at a YSC at a given time, we find more BH–BH binaries at $Z = 0.01\,Z_{\odot}$ than at $Z = 0.1$and $1\,Z_{\odot}$.

Finally, we notice that the first BH–BH binaries form at $t \sim 3$ Myr, i.e. the time of core collapse, regardless of the metallicity. This is a consequence of the fact that binary hardening becomes important during the core collapse and drives the re-expansion of the core (Mapelli & Bressan 2013).

3.2 Lifetimes and exchanges

In Section 3.1, we showed that metal-poor YSCs build up their BH–BH binary population earlier than metal-rich ones. Furthermore, the

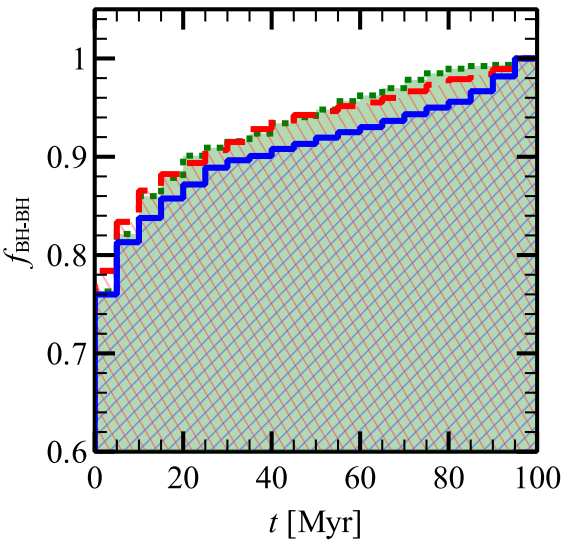

Figure 3. Cumulative distribution of BH–BH binary lifetimes (normalized to the total number of BH–BH binaries per metallicity). Blue diagonally hatched histogram: $Z = 0.01\,Z_{\odot}$; red diagonally hatched histogram: $Z = 0.1\,Z_{\odot}$; green filled histogram: $Z = Z_{\odot}$.

BH–BH binaries that form in metal-poor YSCs ($Z = 0.01\,Z_{\odot}$) are more stable, i.e. have longer lifetimes (before they break up or undergo another exchange). This is a consequence of the higher BH masses allowed in the failed SN scenario. In Fig. 3, we show the cumulative distribution of BH–BH binary lifetimes. At $Z = 0.1$ and $1\,Z_{\odot}$, 90 per cent of BH–BH binaries survive for less than 20 Myr, while at $Z = 0.01\,Z_{\odot}$, 90 per cent of BH–BH binaries survive up to 40 Myr. Furthermore, about 5 per cent of BH–BH binaries survive for more than 80 Myr in the YSCs with $Z = 0.01\,Z_{\odot}$, while only 1–2 per cent of BH–BH binaries survive for more than 80 Myr in the YSCs with $Z \geq 0.1\,Z_{\odot}$.

We have also run a Kolmogorov–Smirnov (KS) test on the distributions presented in Fig. 3. We find a probability $P_{\rm KS} = 4.05 \times 10^{-8}$ that BH–BH binary lifetimes at $Z = 0.01\,Z_{\odot}$ and at $Z = 0.1\,Z_{\odot}$ are drawn from the same distribution. Similarly, $P_{\rm KS} = 5.46 \times 10^{-2}$ when comparing BH–BH binary lifetimes at $Z = 0.01\,Z_{\odot}$ and $Z = Z_{\odot}$, and $P_{\rm KS} = 3.14 \times 10^{-6}$ when comparing BH–BH binary lifetimes at $Z = 0.1\,Z_{\odot}$ and $Z = Z_{\odot}$. This result confirms that the three distributions are statistically different.

We notice that the average number of exchanges is quite the same across different metallicities in Table 2. Thus, the difference in lifetimes must be interpreted as a higher probability of binary break up (i.e. ionization) in case of high metallicity. Also, from Table 2, we notice that the few survived NS–NS binaries are very stable, as they undergo a low number of exchanges.

Table 2. Average number of exchanges per metallicity per DCOB type. Values outside (within parenthesis) refer to all DCOBs (only DCOBs that are considered 'stable' according to the criterion defined in STARLAB; see Portegies Zwart et al. 2001 and our Appendix A).

Type	$0.01\,Z_{\odot}$	$0.1\,Z_{\odot}$	$Z_{\odot}$
BH–BH	9.92 (0.41)	9.91 (0.48)	10.14 (0.58)
NS–NS	0.00 (0.00)	0.50 (0.15)	0.26 (0.09)
NS–BH	6.33 (0.49)	3.72 (0.48)	3.48 (0.43)

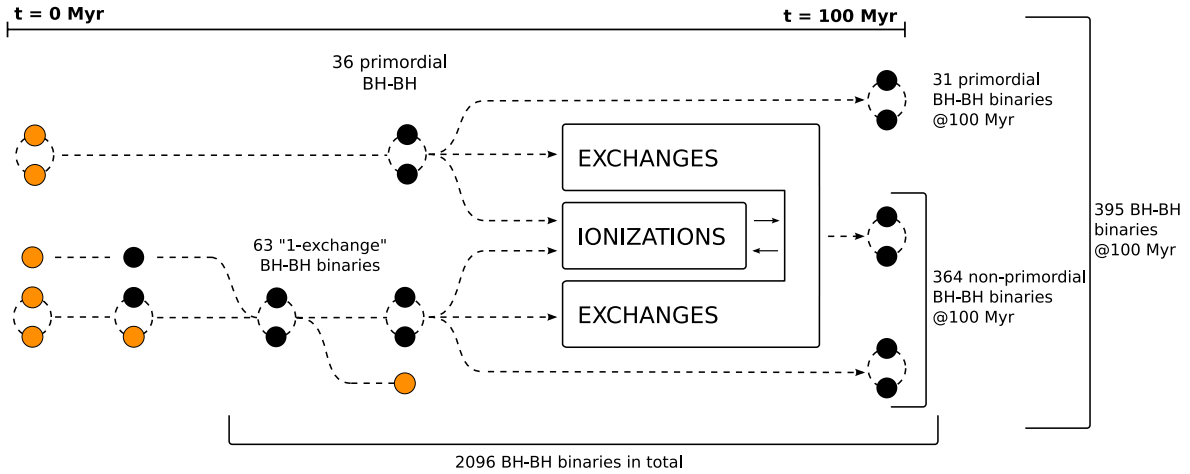

Figure 4. Schematic representation of the main formation and evolution pathways of BH–BH binaries in our simulations. Yellow circles: stars; black circles: BHs. In the top row, from left to right: primordial binaries can evolve into BH–BH binaries by stellar evolution. Then, primordial BH–BH binaries can be ionized or undergo an exchange and become exchanged BH–BH binaries. In the bottom row, from left to right: we call '1-exchange' binaries those BH–BH binaries that form after the exchange of a BH into a BH–star binary. In the following, '1-exchange' binaries can either be ionized or undergo more exchanges. For the sake of simplicity, we call ionizations also the exchanges that transform a BH–BH binary into a BH–star binary. The members of an ionized BH–BH binary can enter a BH–BH binary again via three-body exchange.

Fig. 4 summarizes the possible pathways that lead to the formation of a BH–BH binary and their relative importance in our simulations. BH–BH binaries can derive from either a primordial binary or an exchange. The upper branch of the scheme shows that 36 simulated BH–BH binaries are primordial binaries, while 63 simulated BH–BH binaries form through a dynamical exchange in which a single BH replaces a star in a BH–star binary (in Fig. 4, these systems are called '1-exchange' BH–BH binaries).

In the subsequent evolution, BH–BH binaries born from primordial binaries can either be ionized by a three-body encounter, or undergo an exchange. If the primordial binary undergoes an exchange and if the intruder is a BH, the BH–BH binary becomes an exchanged BH–BH binary. Considering the entire set of simulations for 100 Myr, the total number of BH–BH binaries formed is 2096.

At the end of the simulations (i.e. after 100 Myr), the BH–BH binaries that still survive are 31 primordial binaries and 364 exchanged binaries, for a total of 395 BH–BH binaries (0.66 BH–BH binaries per YSC, on average).

Thus, in summary, 1.7 per cent of all BH–BH binaries in our simulations are primordial binaries, while the remaining 97.3 per cent are exchanged binaries.

3.3 Orbital properties

In Fig. 5, the distributions of the orbital properties of the BH–BH, NS–NS and NS–BH binaries are shown. These are measured at the time in which the semi-major axis a is minimum for each binary. The metallicity does not significantly affect the distribution of semi-major axes and eccentricities of BH–BH binaries. The eccentricity distribution of BH–BH binaries follows the initial equilibrium distribution $f(e) \propto 2e$, but with an excess of low-eccentricity systems coming from the circularization by tidal forces (which influenced some systems before both components collapsed) and by GW emission.

BH–BH binaries span a wide range in both semi-major axes and orbital periods (10^{-2}–10^{6}au and 10^{-3}–10^{7} yr, respectively).

We notice a strong break in the distribution of semi-major axes of BH–BH binaries at $\sim$1 au. This is consistent with the fact that the most massive primordial binaries with separation $a \lesssim 1$ au merged before the formation of BHs, emptying the region of BH–BH binaries with that of semi-major axis. Only dynamical effects can populate this region, but they do it slowly, because the hardening time (i.e. the time-scale for hardening a binary by three-body encounters) scales as a^{-2} (see e.g. Quinlan 1996).

We notice that the softest binaries in Fig. 5 have semi-major axis as large as $\sim$5 pc, close to the initial tidal radius of the YSC. These extremely loose bound pairs are highly unstable (see the discussion in the appendix) and very short lived: it is reasonable to expect that they would completely disappear, if a galactic tidal field would be included in our simulations.

NS–NS binaries are much less numerous than BH–BH binaries (as we showed in Fig. 1), but the distribution of their orbital parameters indicates that NS–NS binaries have generally smaller semi-major axes than BH–BH binaries. This may be due to a selection effect: as NS–NS binary progenitors are often ionized either by natal kicks or by exchanges involving more massive stellar objects (e.g. BHs), only the hardest NS–NS binaries survive in our simulations.

Finally, NS–BH binaries are about 10 times less numerous than BH–BH binaries, but follow approximately the same distribution of orbital parameters.

3.4 Mass distribution

The mass of the BHs affects both the frequency and the amplitude of the GW signal (e.g. Maggiore 2008). Thus, it is important to look at the distribution of the masses of the simulated BH–BH binaries.

Fig. 6 shows the distribution of m_1, m_2 and of the chirp mass $m_{\rm chirp}$. The chirp mass is defined as $m_{\rm chirp} = (m_1\, m_2)^{3/5}/(m_1 + m_2)^{1/5}$. The chirp mass is named so because it is this combination of m_1 and m_2 that determines how fast the binary sweeps, or chirps, through a frequency band. In fact, it can be shown that the amplitude and the frequency of GWs scale as $m_{\rm chirp}^{5/3}$ and $m_{\rm chirp}^{-5/8}$, respectively (Maggiore 2008).

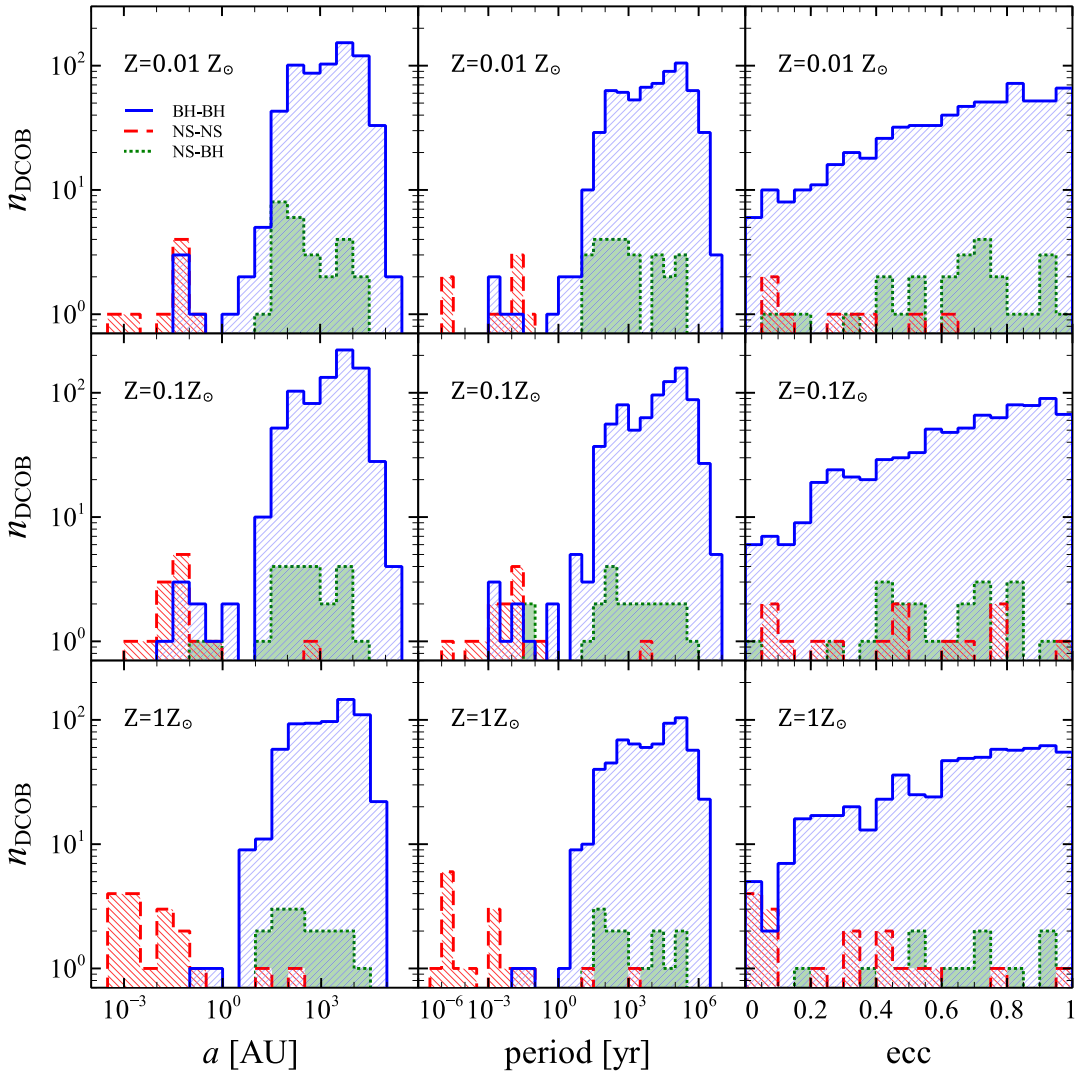

Figure 5. Histograms of the orbital properties of DCOBs measured, for each binary, when the semi-major axis a is minimum. Columns from left to right refer to semi-major axis a, period and eccentricity of the binary. Rows from top to bottom refer to three different metallicities: $Z = 0.01, 0.1$ and $1\,Z_{\odot}$. The blue, red and green histograms refer to BH–BH, NS–NS and NS–BH binaries, respectively.

The mass of the primary (secondary) can be as high as $85\,M_{\odot}$ ($78\,M_{\odot}$) in case of $Z = 0.01\,Z_{\odot}$. Such large values correspond to BHs that formed from direct collapse (see Section 2 and Paper I).

We also found a $73\,M_{\odot}$ BH at $Z = Z_{\odot}$, i.e. a much higher mass than expected from stellar evolution of isolated stars with solar metallicity. This BH is the result of a dynamically induced merger between a smaller BH ($14.9\,M_{\odot}$) and a star ($59.3\,M_{\odot}$).

Chirp masses are very high, too. The black histogram in Fig. 6 shows the chirp mass distribution of our best BH–BH merger candidates (i.e. of those systems that are expected to merge within a Hubble time, see next section for details): we notice that one of these systems has a significantly high chirp mass ($m_{\rm chirp} \simeq 40\,M_{\odot}$).

The GW searches for BH–BH binaries performed by LIGO and VIRGO (Abadie et al. 2012a; Aasi et al. 2013) cover the mass range found by the present simulation. The signal corresponding to our higher chirp masses can be detected by the Intermediate Mass Binary Black Holes search (Abadie et al. 2012b).

In the adopted model, the chirp mass strongly depends on the metallicity of the progenitor stars. Since the amplitude and the frequency of GWs scale as $m_{\rm chirp}^{5/3}$ and $m_{\rm chirp}^{-5/8}$, respectively, it will be possible to link the observed GW signal to the chirp mass of the source. Observing large chirp masses would be clear evidence for the scenario of BH birth and evolution in the low-metallicity environments.

3.5 Coalescence time-scale

The time-scale for coalescence (Peters 1964) is defined as

$$t_{\rm GW} = \frac{5}{256}\frac{c^5\,a^4\,(1-e^2)^{7/2}}{G^3\,m_1\,m_2\,(m_1+m_2)}, \qquad (2)$$

where c is the speed of light and G the gravitational constant. $t_{\rm GW}$ is the time-scale for a binary to merge by GW emission. It scales as a^4, and it is shorter for high eccentricity. GW emission affects the coalescence time-scale by shrinking the semi-major axis and circularizing the binary orbit. Fig. 7 shows $t_{\rm GW}$ as a function of semi-major axis, eccentricity and metallicity of the simulated systems.

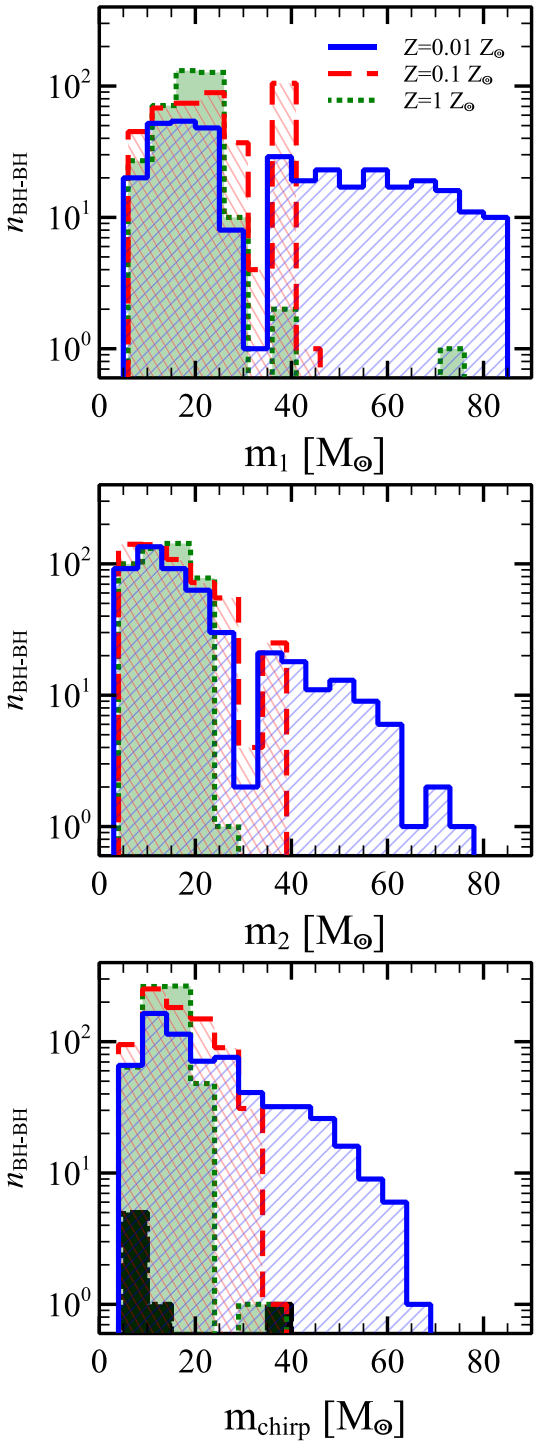

Figure 6. From top to bottom: distribution of the primary component, the secondary component and the chirp mass of BH–BH binaries, respectively. In each panel, the blue, red and green histograms correspond to $Z = 0.01, 0.1, 1\,Z_{\odot}$, respectively. In the bottom panel, the black histograms show the distribution of chirp masses of the seven BH–BH binaries that are expected to merge within a Hubble time (see Section 3.5).

Most of the systems with $t_{\rm GW} \leq t_{\rm H}$ (where $t_{\rm H} = 13$ Gyr is the Hubble time) have eccentricity close to zero, as a consequence of circularization by GW emission. However, we found an outlier (with eccentricity $e = 0.997$, see Table 3) produced by dynamical exchange. This is interesting not only because its coalescence time-scale is short, due to the high value of the eccentricity, but also because it suggests that the use of templates which include eccentric effects in the LIGO and VIRGO searches could be important (Brown & Zimmerman 2010). Unfortunately, this binary is destroyed by a new dynamical exchange before it merges. On the other hand, we expect to find other systems like this with a larger simulation sample, and we cannot exclude that some of them can evolve (without being destroyed by further exchanges) till they merge. Such systems would be very important for GW detection (Brown & Zimmerman 2010; Samsing, MacLeod & Ramirez-Ruiz 2014).

Table 3. List of the BH–BH binaries with coalescence time-scale <13 Gyr, in ascending order of coalescence time-scale. Column 1: coalescence time-scale in Gyr; column 2: semi-major axis in au; column 3: period in years; column 4: eccentricity; column 5: metallicity; column 6: whether or not (Y/N) the binary merges during the simulation.

$t_{\rm GW}$ (Gyr)	a (au)	P (yr)	ecc	$Z\,(Z_{\odot})$	Merger
0.09	7.77	2.277 88	0.997	0.01	N
0.20	0.03	0.001 07	0.019	0.1	N
0.67	0.04	0.001 96	0.019	0.1	N
1.34	0.05	0.002 67	0.019	0.01	N
1.49	0.05	0.002 76	0.014	0.1	N
1.76	0.05	0.002 96	0.028	0.01	N
2.06	0.07	0.003 87	0.016	0.01	N

All BH–BH binaries with $t_{\rm GW} \leq t_{\rm H}$ are at low metallicity ($Z = 0.01$ and $0.1\,Z_{\odot}$), while we find none at solar metallicity. The bottom panels in Fig. 7 show the coalescence time-scale for NS–NS binaries. The total number of NS–NS binaries is much smaller than that of BH–BH binaries but they are much harder. As a consequence, their coalescence time-scales are generally shorter. The minimum coalescence time-scale for BH–BH binaries in our simulations is $t_{\rm GW} \sim 0.1$ Gyr, while that for NS–NS binaries is $t_{\rm GW} \sim 10^{-5}$ Gyr. We also found that 11 NS–NS binaries actually merged before 100 Myr.

In the bottom panel of Fig. 7, we also show the coalescence time-scale for NS–BH binaries. No NS–BH mergers are expected in less than a Hubble time, because NS–BH binaries are much less numerous than BH–BH binaries and they are not favoured by dynamical encounters.

Tables 3 and 4 list the shortest coalescence time-scales for BH–BH binaries and NS–NS binaries, respectively.

It has been debated (e.g. Clausen et al. 2013) whether $t_{\rm GW}$ is a reliable indicator of the merger time-scale in star clusters. In fact, dynamical interactions in star clusters may affect the evolution of a DCOB and delay or anticipate the merger with respect to the expected $t_{\rm GW}$. In our simulations, there is good agreement between the coalescence time-scales and the actual mergers; thus, we can conclude that in most cases dynamics does not affect the actual merger time-scale of the simulated NS–NS binaries.

4 DISCUSSION

4.1 Estimate of the merger rate

Since most stars form in YSCs, the mass density of YSCs in the Universe is expected to scale as the star formation rate (SFR) density (Mapelli et al. 2010b). Thus, from the results discussed in Section 3.5 and using a Drake-like equation, the merger rate of BH–BH

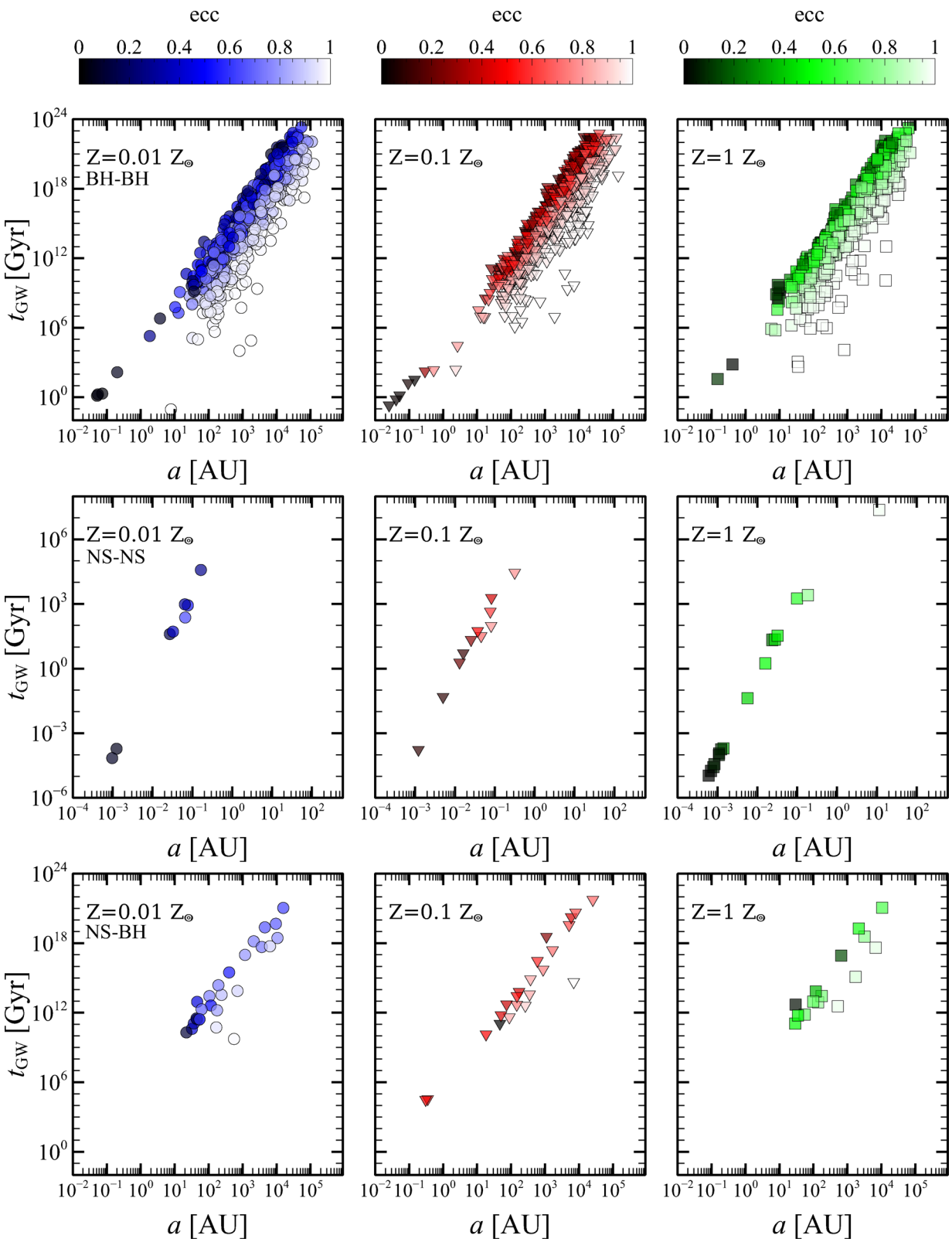

Figure 7. Coalescence time-scale as a function of the semi-major axis for BH–BH binaries, NS–NS binaries and NS–BH from top to bottom. From left to right: metallicity $Z = 0.01$ (blue circles), 0.1 (red triangles) and $1\,Z_{\odot}$ (green squares). The colour-coded map refers to eccentricity.

Table 4. List of NS–NS binaries with coalescence time <13 Gyr, in ascending order of coalescence time-scale. Column 1: coalescence time-scale in Myr; column 2: semi-major axis in units of 10^{-3} au; column 3: period in units of 10^{-5} yr; column 4: eccentricity; column 5: metallicity; column 6: whether or not (Y/N) the binary merges during the simulation. The minimum, mean and maximum difference between the real merger and the coalescence times are 0.02, 0.24 and 0.12 Myr, respectively.

$t_{\rm GW}$ (Myr)	a (10^{-3} au)	P (10^{-5} yr)	ecc	Z ($Z_\odot$)	Merger
0.01	0.60	0.9	0.005	1	Y
0.02	0.69	1.1	0.01	1	Y
0.03	0.79	1.4	0.05	1	Y
0.04	0.84	1.5	0.05	1	Y
0.07	0.97	1.9	0.08	0.01	Y
0.1	1.09	2.2	0.06	1	Y
0.1	1.1	2.4	0.03	1	Y
0.2	1.2	2.7	0.09	0.1	Y
0.2	1.2	2.7	0.08	1	Y
0.2	1.3	2.8	0.06	0.01	Y
0.2	1.4	3.3	0.31	1	Y
40	5.7	26.9	0.42	1	N
50	5.0	22.3	0.09	0.1	N
1760	20	12.5	0.51	1	N
1960	10	93.4	0.21	0.1	N
5330	20	13.0	0.11	0.1	N

binaries can be estimated as

$$R_{\rm BH-BH} = N_{\rm mrgr,\,BH-BH} \quad \rho_{\rm SF} \quad t_{\rm life} \quad f_{\rm SF} = 3.5\times10^{-3}\,{\rm Mpc^{-3}\,Myr^{-1}} \left[\frac{N_{\rm mrgr,\,BH-BH}}{3\times10^{-15}\,{\rm M_\odot}^{-1}\,{\rm yr^{-1}}}\right] \left(\frac{\rho_{\rm SF}}{1.5\times10^{-2}\,{\rm M_\odot\,yr^{-1}\,Mpc^{-3}}}\right) \left(\frac{t_{\rm life}}{10^8\,{\rm yr}}\right) \left(\frac{f_{\rm SF}}{0.8}\right), \quad (3)$$

where $\rho_{\rm SF}$ is the cosmological density of SFR at redshift zero ($\rho_{\rm SF} = 1.5\times10^{-2}\,{\rm M_\odot\,yr^{-1}\,Mpc^{-3}}$ from Hopkins & Beacom 2006), $t_{\rm life}$ is the average lifetime of a YSC, $f_{\rm SF}$ is the fraction of star formation (SF) that occurs in YSCs (we take $f_{\rm SF} = 0.8$ from Lada & Lada 2003) and $N_{\rm mrgr,\,BH-BH}$ is the number of BH–BH binary mergers per solar mass per year, as estimated from our simulations (see Table 3). In equation (3), we assume that $R_{\rm BH-BH}$ does not change significantly with time. This approximation is reasonable for the distance range of Advanced LIGO and VIRGO (see the short discussion at the end of this section).

Equation (3) has been derived following the same approach as explained in Mapelli et al. (2010a, see also Mapelli et al. 2012). The main differences between equation (3) of this paper and equations 2 and 3 of Mapelli et al. (2010b) are the following: (i) in equation (3), we just estimate the merger rate, while Mapelli et al. (2010b) estimate the detection rate for different interferometers; (ii) in equation (3), we derive $N_{\rm mrgr,\,BH-BH}$ directly from our simulations, while in Mapelli et al. (2010b), we used the results of a toy model for intermediate-mass BHs.

In particular, we estimate $N_{\rm mrgr,\,BH-BH}$ as

$$N_{\rm mrgr,\,BH-BH} = 3\times10^{-15}\,{\rm M_\odot}^{-1}\,{\rm yr^{-1}} \left(\frac{N_{\rm exp,\,BH-BH}}{3}\right) \left(\frac{200}{N_{\rm YSC}}\right) \left(\frac{3500\,{\rm M_\odot}}{\langle M_{\rm TOT}\rangle}\right) \left(\frac{1.5\,{\rm Gyr}}{t_{\rm GW,\,max}}\right), \quad (4)$$

where $N_{\rm YSC}$ is the number of simulated YSCs, $\langle M_{\rm TOT}\rangle$ is the average mass of a single YSC[2] and $N_{\rm exp,\,BH-BH}$ is the number of BH–BH binaries that are expected to merge within a time $t_{\rm GW,\,max}$. For example, at $Z = 0.1\,{\rm Z_\odot}$, we find that three BH–BH binaries are expected to merge within $t_{\rm GW,\,max} = 1.5$ Gyr (see Table 3). At $Z = 0.01\,{\rm Z_\odot}$, we find that four BH–BH binaries are expected to merge within $t_{\rm GW,\,max} = 2.1$ Gyr, while at $Z = 1\,{\rm Z_\odot}$, we do not find any BH–BH binaries that merge within $t_{\rm GW,\,max} = t_{\rm H}$. Thus, we find that $0 \leq N_{\rm mrgr,\,BH-BH} \leq 3\times10^{-15}\,{\rm M_\odot}^{-1}\,{\rm yr^{-1}}$ depending on the metallicity. The resulting values of the merger rate are $R_{\rm BH-BH} = 0$, 3.3 and $3.5\times10^{-3}\,{\rm Mpc^{-3}\,Myr^{-1}}$, if we assume that all YSCs in the local Universe have metallicity 1, 0.1 and $0.01\,{\rm Z_\odot}$, respectively.

Thus, the merger rate of BH–BH binaries is $R_{\rm BH-BH} \sim 3.5\times10^{-3}\,{\rm Mpc^{-3}\,Myr^{-1}}$ if we assume that all YSCs in the local Universe formed at low metallicity ($Z \leq 0.1\,{\rm Z_\odot}$), and is $R_{\rm BH-BH} \sim 0$ if we assume that all YSCs in the local Universe formed at high metallicity ($Z = {\rm Z_\odot}$), since in our simulations we did not find any BH–BH binary at $Z = {\rm Z_\odot}$ with coalescence time-scale shorter than the Hubble time. Even if the statistics is low, this result is important, as we can conclude that BH–BH binaries are enhanced at low metallicity, where more massive BHs can form.

As a first-order approximation, we can assume that the merger rate of BH–BH binaries in the local Universe is included in this range of values, i.e. $0 \leq R_{\rm BH-BH} \leq 3.5\times10^{-3}\,{\rm Mpc^{-3}\,Myr^{-1}}$. For a more realistic assumption about the metallicity of YSCs in the local Universe, see the discussion at the end of this section.

Similarly, the merger rate of NS–NS binaries can be estimated as

$$R_{\rm NS-NS} = N_{\rm mrgr,\,NS-NS} \quad \rho_{\rm SF} \quad t_{\rm life} \quad f_{\rm SF} = 0.15\,{\rm Mpc^{-3}\,Myr^{-1}} \left[\frac{N_{\rm mrgr,\,NS-NS}}{1.3\times10^{-13}\,{\rm M_\odot}^{-1}\,{\rm yr^{-1}}}\right] \left(\frac{\rho_{\rm SF}}{1.5\times10^{-2}\,{\rm M_\odot\,yr^{-1}\,Mpc^{-3}}}\right) \left(\frac{t_{\rm life}}{10^8\,{\rm yr}}\right) \left(\frac{f_{\rm SF}}{0.8}\right), \quad (5)$$

where $N_{\rm mrgr,\,NS-NS}$ is the number of NS–NS binary mergers per solar mass per year and can be derived as

$$N_{\rm mrgr,\,NS-NS} = 1.3\times10^{-13}{\rm M_\odot}^{-1}\,{\rm yr^{-1}} \left(\frac{N_{\rm exp,\,NS-NS}}{9}\right) \left(\frac{200}{N_{\rm YSC}}\right) \left(\frac{3500\,{\rm M_\odot}}{\langle M_{\rm TOT}\rangle}\right) \left(\frac{100\,{\rm Myr}}{t_{\rm life}}\right), \quad (6)$$

where $N_{\rm exp,\,NS-NS}$ is the number of NS–NS binaries that actually merged during our simulations and $t_{\rm life} = 100$ Myr is the assumed YSC life (and the duration of the simulation). In the case of NS–NS binaries, we use the number of merged binaries (rather than the number of expected mergers, as in the case of BH–BH binaries), because we have sufficient statistics to do so. At $Z = 1, 0.1$ and $0.01\,{\rm Z_\odot}$ $N_{\rm exp,\,NS-NS} = 9,\ 2,\ 2$, respectively.

Thus, the merger rate of NS–NS binaries is $R_{\rm NS-NS} \sim 0.15\,{\rm Mpc^{-3}\,Myr^{-1}}$ if we assume that all YSCs in the local Universe formed at high metallicity ($Z = {\rm Z_\odot}$, see Table 4), and is $R_{\rm NS-NS} \sim 0.03\,{\rm Mpc^{-3}\,Myr^{-1}}$ if we assume that all YSCs in the local Universe formed low metallicity ($Z = 0.01, 0.1\,{\rm Z_\odot}$). This is

[2] Since we simulated only YSCs with $M_{\rm TOT} \sim 3500\,{\rm M_\odot}$, equation (4) suffers from the approximation that we do not consider a mass spectrum for the simulated YSCs. On the other hand, YSCs with $M_{\rm TOT} \sim 3500\,{\rm M_\odot}$ are among the most diffuse YSCs in the local Universe (Lada & Lada 2003). In a forthcoming paper, we will consider a mass spectrum for the YSCs.

another important result of our simulations, as it implies that NS–NS mergers are suppressed at low metallicity.

As a first-order approximation, we can assume that the merger rate of NS–NS binaries in the local Universe is included in this range of values, i.e. $0.03\,\mathrm{Mpc^{-3}\,Myr^{-1}} \leq R_{\mathrm{NS-NS}} \leq 0.15\,\mathrm{Mpc^{-3}\,Myr^{-1}}$. In equation (5), we assume that $R_{\mathrm{NS-NS}}$ does not change significantly with time. This approximation is reasonable for the distance range of Advanced LIGO and VIRGO (see the short discussion at the end of this section).

Finally, the merger rate of NS–BH binaries is $R_{\mathrm{NS-BH}} < 10^{-4}\,\mathrm{Mpc^{-3}\,Myr^{-1}}$ for all considered metallicities, as we found no simulated systems with coalescence time-scale shorter than the Hubble time. In our simulations, NS–BH systems are much less common than BH–BH binaries, since the latter are favoured by dynamical exchanges with respect to the former.

Our estimates of the merger rate show that there is a possible trend with metallicity: the mergers of NS–NS binaries are favoured at high metallicity ($\sim Z_{\odot}$), while the mergers of BH–BH binaries are more frequent at low metallicity ($\sim 0.01-0.1\,Z_{\odot}$). We recall that $Z = 0.01\,Z_{\odot}$ is the typical metallicity of GCs in the Milky Way (e.g. Harris 1996), $Z = 0.1\,Z_{\odot}$ is the metallicity of many irregular galaxies and dwarf galaxies in the local Universe (e.g. Mapelli et al. 2010a), while a metallicity close to solar is normally found in the bulges of giant spiral galaxies and elliptical galaxies (e.g. Pilyugin, Vílchez & Contini 2004). Furthermore, a metallicity gradient (with Z decreasing at larger distance from the centre) has been found in most local late-type galaxies (Pilyugin et al. 2004). Thus, the metallicity of the local Universe is quite patchy, with a preference for higher metallicity at the centre of the most massive galaxies and for lower metallicity in the outskirts of massive galaxies as well as in dwarf and irregular galaxies.

Furthermore, the Sloan Digital Sky Survey shows that the SF in the last Gyr has a bimodal distribution: about half of it occurs at solar metallicity, while the remaining half takes place at $Z \sim 0.1\,Z_{\odot}$ (Panter et al. 2008). Therefore, we expect that about half of the YSCs that formed in the last Gyr have $Z \sim Z_{\odot}$, while the remaining half have $Z \sim 0.1\,Z_{\odot}$. In contrast, a negligible fraction of YSCs formed at $Z = 0.01\,Z_{\odot}$ in the last Gyr.

If we assume (as suggested by Panter et al. 2008) that half of the YSCs that formed in the last Gyr have $Z \sim Z_{\odot}$, while the remaining half have $Z \sim 0.1\,Z_{\odot}$, the rate of mergers we expect today from our simulated YSCs (using equations 5 and 3) is $R_{\mathrm{NS-NS}} \sim 0.10\,\mathrm{Mpc^{-3}\,Myr^{-1}}$ and $R_{\mathrm{BH-BH}} \sim 1.7 \times 10^{-3}\,\mathrm{Mpc^{-3}\,Myr^{-1}}$, for NS–NS and BH–BH binaries, respectively.

The aforementioned values of $R_{\mathrm{NS-NS}}$ and $R_{\mathrm{BH-BH}}$ have been derived from the typical properties of YSCs in the local Universe and assuming a metallicity mixture valid for the last Gyr (i.e. up to redshift $z \sim 0.1$). Are they valid over the entire distance range of Advanced LIGO and VIRGO? According to Abadie et al. (2010), the distance range of Advanced LIGO and VIRGO will be $\sim$200 Mpc ($z \sim 0.05$) and 1 Gpc ($z \sim 0.2$) for NS–NS and BH–BH mergers, respectively. Thus, we can conclude that our estimated merger rates are fairly uniform (within the uncertainties) across the range of Advanced LIGO and VIRGO, especially in the case of NS–NS mergers.

We recall that the DCOBs that form in YSCs will be ejected to the field as a consequence of evaporation, natal kicks and three-body encounters, and because of the disruption of the parent YSCs by the tidal field of the host galaxy. Thus, the merger rate we estimate in this section represents the expected merger rate for the field. This is very important, as previous studies estimated the merger rate either for long-lived GCs (e.g. O'Leary et al. 2006; Downing et al. 2010, 2011) or for the field (e.g. Belczynski et al. 2010a; Dominik et al. 2012, 2013). In previous work, the effect of dynamics has been included only in the estimate of the merger rate within GCs, while field binaries have been assumed to form and evolve in isolation (through population synthesis codes). On the other hand, it is well known that most stars form in YSCs and evolve dynamically via three-body encounters, before being ejected into the field. Our results show that the estimate of the merger rate in the field should account for dynamical evolution.

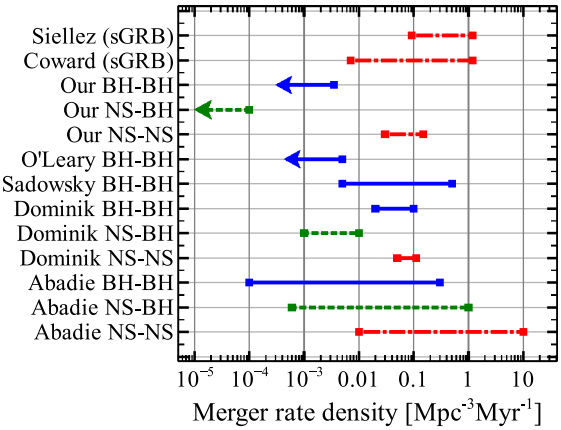

Figure 8. Comparison of our predictions for the merger rates of NS–NS, NS–BH and BH–BH binaries with some of the most representative estimates available in the literature. From top to bottom: Siellez, Boër & Gendre (2014); Coward et al. (2012); our paper; O'Leary et al. (2006); Sadowski et al. (2008); Dominik et al. (2013) and Abadie et al. (2010). The predicted merger rates for Dominik et al. (2013) span from their 'standard' to their 'optimistic CE' model (see fig. 1 in Dominik et al. 2013).

4.2 Comparison with previous work

Fig. 8 compares our predictions of the merger rates with some of the most representative estimates available in the literature. From this figure, it is apparent that our prediction of $R_{\mathrm{NS-NS}}$ is fairly consistent with the estimate derived from short gamma-ray bursts (Coward et al. 2012; Siellez et al. 2014).

Furthermore, our results for $R_{\mathrm{NS-NS}}$ and $R_{\mathrm{BH-BH}}$ are consistent with the estimates provided in Abadie et al. (2010). In contrast, our results for $R_{\mathrm{NS-BH}}$ are significantly lower than predicted by Abadie et al. (2010). We recall that the value of $R_{\mathrm{NS-NS}}$ reported by Abadie et al. (2010) is derived from the observed rate of NS–NS binaries in the Milky Way (Kalogera et al. 2004), while the values of $R_{\mathrm{NS-BH}}$ and $R_{\mathrm{BH-BH}}$ are obtained from population synthesis codes (O'Shaughnessy et al. 2008 and Kalogera et al. 2007, respectively) and are only indirectly constrained by the SN rate.

The main differences between the approach presented in Abadie et al. (2010) and ours are the following: (i) the estimates presented in Abadie et al. (2010) are based on population synthesis simulations of isolated binaries and do not account for the fact that most stars form in YSCs; (ii) the mass spectrum of BHs is significantly different; (iii) Abadie et al. (2010) assume that most galaxies in the local Universe are Milky Way analogues, while in this paper, we adopt the cosmic SFR by Hopkins & Beacom (2006). The fact that we account for the dynamical evolution of YSCs and include more massive BHs than Abadie et al. (2010) affects the results significantly, as the formation of BH–BH binaries is enhanced with respect to that of NS–BH systems. In general, our simulated DCOBs cannot evolve in

isolation but frequently undergo three-body encounters that perturb their orbits, while the results of Abadie et al. (2010) are obtained assuming that all binaries evolve in isolation.

Recent studies by Belczynski et al. (2010a), Dominik et al. (2012) and Dominik et al. (2013) adopt a BH mass spectrum much more similar to ours and investigate the dependence of the merger rate on metallicity, even if they do not include three-body encounters. As a consequence, the distribution of BH–BH binary chirp masses in the three aforementioned papers is very similar to our distribution. The main difference is the absence of massive BHs that come from a merger in the papers by Belczynski et al. (2010a), Dominik et al. (2012) and Dominik et al. (2013), because they do not allow merged binaries to acquire a new companion dynamically.

In their standard model, Dominik et al. (2013) find an estimate of $R_{\rm NS-NS}$ that is fairly consistent with ours, while their prediction for $R_{\rm NS-BH}$ and $R_{\rm BH-BH}$ are about a factor of 10 higher. In addition, Belczynski et al. (2010a), Dominik et al. (2012) and Dominik et al. (2013) present an alternative model in which common envelope (CE) phases on the Hertzsprung gap are allowed (i.e. the binary is not assumed to merge when one of the two members reaches the Hertzsprung gap). The merger rates obtained with this assumption are a factor of $\geq$100 higher than our results. This discrepancy is consistent with our expectations, as our simulations adopt the same recipes for the CE phase as in the standard model of Dominik et al. (2013)[3].

Sadowski et al. (2008) study the merger rate of DCOBs in GCs and in the field by means of Monte Carlo simulations and population synthesis models, respectively. They find that NS–NS binaries and NS–BH binaries should dominate the DCOB population in the field, whereas BH–BH binaries are the main merger candidates in GCs. We confirm their result, in the sense that the formation of BH–BH binaries is enhanced by dynamics in star clusters. Our results agree with those of Sadowski et al. (2008) also for the importance of dynamical exchanges: Sadowski et al. (2008) find that 6 per cent (94 per cent) of BH–BH binary merger candidates come from primordial binaries (dynamical exchanges), while we find that 1.7 per cent of our BH–BH binaries come from primordial binaries.

On the other hand, Sadowski et al. (2008) neglect the fact that many of the merger candidates in the field have been ejected from YSCs (by dynamical ejection, natal kick or YSC disruption). Accounting for field DCOBs that were ejected from YSCs increases the relative importance of BH–BH binaries in the field, especially at low metallicity. Furthermore, Sadowski et al. (2008) find a merger rate $R_{\rm BH-BH} \sim 0.005-0.5$ Mpc^{-3} Myr^{-1} in dense star clusters, substantially higher than our result ($R_{\rm BH-BH} \leq 0.0035$ Mpc^{-3} Myr^{-1}), because they assume that the BHs remain in dynamical equilibrium with the rest of the cluster. This suppresses the dynamical ejection of BHs.

Other recent papers (O'Leary et al. 2006; Downing et al. 2010, 2011; Clausen et al. 2013) focus on DCOB merger in dense stellar systems and GCs. In particular, O'Leary et al. (2006) perform Monte Carlo simulations of GCs in which they assume that the BH population is concentrated in the core and dynamically decoupled from the rest of the cluster, because of the Spitzer instability (Spitzer 1969). O'Leary et al. (2006) find that most BH–BH binaries are ejected from the parent star cluster and that the resulting merger rate is $R_{\rm BH-BH} \leq 0.005$ Mpc^{-3} Myr^{-1}, much lower than in Sadowski et al. (2008), because of the assumed Spitzer instability. The merger rate estimated by O'Leary et al. (2006) is very similar to our result.

Downing et al. (2010) and Downing et al. (2011) perform Monte Carlo simulations of GCs. They (i) include a treatment of metallicity that is close to ours (even if their maximum BH mass is generally lower than ours, as they use the same distribution as in Belczynski et al. 2006), (ii) assume neither Spitzer instability nor rigid equilibrium between the BHs and the rest of the cluster a priori. Downing et al. (2010) find that the BHs strongly mass segregate and evolve similarly to what was assumed by O'Leary et al. (2006). Downing et al. (2010) find an even lower merger rate than the one derived by O'Leary et al. (2006) and by our paper, but they admit that this may be due to their approximate treatment of three-body encounters. On the other hand, the distribution of orbital periods in the simulations by Downing et al. (2010) is similar to ours (see Fig. 5). Furthermore, both this paper and Downing et al. (2010) find that most BH–BH binaries form dynamically, through exchanges. Finally, Downing et al. (2010) find that BH–BH binaries form earlier and are more stable at low metallicity, because BHs are more massive, in agreement with our results (see Figs 2 and 3).

In conclusion, our results confirm that most BH–BH binaries in star clusters come from dynamical exchanges, in agreement with the findings of Monte Carlo simulations of dense star clusters (O'Leary et al. 2006; Downing et al. 2010, 2011). On the other hand, our simulated star clusters are a factor of 10−1000 less massive and a factor of $\geq$5 smaller than those studied in previous work (e.g. Downing et al. 2010). Thus, they are expected to be much more numerous in the local Universe than those considered by previous work (since the mass function of YSCs scales as $M_{\rm TOT}^{-2}$; Lada & Lada 2003). Furthermore, the dynamical evolution time-scale of our simulated YSCs is much shorter, as $t_{\rm rlx} \sim 10\,{\rm Myr}\,(r_{\rm hm}/0.8\,{\rm pc})^{3/2}\,(M_{\rm TOT}/3500\,{\rm M}_\odot)^{1/2}$. Thus, most DCOBs that form in our simulated YSCs will be ejected to the field (by YSC evaporation, three-body encounters or tidal fields) over a time-scale much shorter than found in previous work. Therefore, our YSCs can be considered as the building blocks of the galaxy disc, and the merger rate we have estimated represents the expected merger rate of the field population.

5 CONCLUSIONS

We studied the impact of metallicity and dynamics on the formation and evolution of DCOBs. To this purpose, we have run 600 *N*-body realizations of YSCs chosen to match the properties of the most common YSCs in our Galaxy. We simulated YSCs, because most stars form in YSCs. Thus, we cannot study the formation and evolution of DCOBs without accounting for the fact that most of them originate in YSCs.

For our simulations, we used an upgraded version of the public code STARLAB, which includes recipes for metallicity-dependent stellar evolution and winds, and which allows stars with final mass larger than 40 M$_\odot$ to directly collapse to a BH. Direct collapse leads to the formation of massive stellar BHs ($\geq$ 25 M$_\odot$) at low metallicity.

We found that, while the number of NSs is about four times larger than the number of BHs, the number of BH–BH binaries is about 10 times higher than the number of NS–NS binaries. The reason is that dynamical interactions enhance the formation of BH–BH binaries with respect to NS–NS binaries. Heavier BHs sink to the centre of the YSC, where they are more likely to interact with other

[3] As discussed in Paper I, we adopt $\alpha_{\rm CE}\,\lambda = 0.5$ to model the CE phase (see Davis, Kolb & Knigge 2012, for a definition), and we assume that all binaries that enter a CE phase when at least one of the two members is in the Hertzsprung gap merge.

BHs: BHs can acquire companions through three-body exchanges. Since the probability of a dynamical exchange is higher when the single star is more massive than one of the members of the binary and since BHs are among the most massive objects in a YSC, exchanges favour the formation of BH–BH binaries.

BH–BH binaries form earlier at low metallicity, because BHs are more massive in metal-poor YSCs. Furthermore, BH–BH binaries formed at low metallicity are more stable: they live longer than BH–BH binaries in metal-rich YSCs.

The simulated BH–BH binaries have very large chirp masses ($5-70\ M_{\odot}$), because of the direct collapse at low metallicity and because mergers between stars and BHs are allowed.

BH–BH binaries span a wide range in periods (10^{-3}–10^{7} yr). In contrast, most NS–NS binaries have periods <1 yr. As a consequence, the coalescence time-scale is generally longer for BH–BH binaries than for NS–NS binaries. The minimum coalescence time-scale for BH–BH binaries and NS–NS binaries is $t_{\rm GW} \sim 0.1$ Gyr and $t_{\rm GW} \sim 10^{-5}$ Gyr, respectively. Only seven BH–BH binaries are expected to merge within a Hubble time. Moreover, no BH–BH binaries merge during our simulations, while 11 NS–NS binaries do.

From our simulations, we can estimate the merger rate of DCOBs in the local Universe. We find a merger rate $R_{\rm BH-BH} \leq 3.5 \times 10^{-3}\,{\rm Mpc^{-3}\,Myr^{-1}}$, $R_{\rm NS-BH} < 10^{-4}\,{\rm Mpc^{-3}\,Myr^{-1}}$ and $R_{\rm NS-NS} \sim 0.03-0.15\,{\rm Mpc^{-3}\,Myr^{-1}}$ for BH–BH, NS–BH and NS–NS binaries, respectively. The merger rate of NS–NS binaries is fairly consistent with the estimates based on both the observed Galactic NS–NS binaries (Kalogera et al. 2004) and the observed rate of short gamma-ray bursts (Coward et al. 2012; Siellez et al. 2014). The merger rate of BH–BH binaries is consistent with recent Monte Carlo simulations of dense star clusters (e.g. O'Leary et al. 2006; Downing et al. 2010). The merger rate of NS–BH binaries is quite low with respect to previous estimates based on population synthesis codes (e.g. O'Shaughnessy et al. 2008). This can be explained with the fact that the formation of NS–BH binaries is less favoured by dynamical exchanges than the formation of BH–BH binaries.

Our merger rates are still affected by a number of assumptions that will be improved in forthcoming studies. First, in our study, we assume that the lifetime of the simulated YSCs is 100 Myr, but we do not take into account the presence of a realistic galactic tidal field. Secondly, we explore only a limited portion of the parameter space. In forthcoming studies, we will consider YSCs with different concentration, half-mass radius, total mass and binary fraction.

Our simulated YSCs are expected to dissolve in the galactic disc in $\sim$100 Myr, which is much shorter than the coalescence time-scale of all BH–BH binaries and of some NS–NS binaries. The DCOBs that form within the simulated YSCs are ejected in the field (due to three-body interactions or because of the disruption of the parent YSC). Once in the field, the DCOBs will not undergo more dynamical interactions and will continue their evolution in isolation, until they merge. Thus, the mergers of (most) our simulated DCOBs are expected to take place in the field. Accounting for the fact that most DCOBs form in YSCs and evolve through dynamical interactions is a crucial step towards obtaining a realistic description of the demographics of DCOBs, in light of the forthcoming Advanced LIGO and VIRGO scientific runs.

ACKNOWLEDGEMENTS

We thank the referee Matthew Benacquista for the careful reading and the constructive comments which helped us to improve the manuscript. We also thank Alessandra Mastrobuono Battisti and Roberto Soria for useful discussions. We made use of the public software package STARLAB (version 4.4.4) and of the SAPPORO library (Gaburov, Harfst & Portegies Zwart 2009) to run STARLAB on graphics processing units (GPUs). We acknowledge all the developers of STARLAB, and especially its primary authors: Piet Hut, Steve McMillan, Jun Makino and Simon Portegies Zwart. We thank the authors of SAPPORO, and in particular E. Gaburov, S. Harfst and S. Portegies Zwart. BMZ, MM and MB acknowledge financial support from the Italian Ministry of Education, University and Research (MIUR) through grant FIRB 2012 RBFR12PM1F. BMZ was supported by a PhD fellowship from Padova University through the Strategic Research Project AACSE (Algorithms and Architectures for Computational Science and Engineering). MM acknowledges financial support from INAF through grant PRIN-2011-1 and from CONACyT through grant 169554. We also acknowledge the CINECA Award N. HP10B3BJEW, HP10CLI3BX, HP10CXB7O8, HP10C894X7, HP10CGUBV0, HP10CP6XSO and HP10C3ANJY for the availability of high-performance computing resources and support.

REFERENCES

Aasi J. et al., 2013, Phys. Rev. D, 87, 022002
Abadie J. et al., 2010, Class. Quantum Gravity, 27, 173001
Abadie J. et al., 2012a, Phys. Rev. D, 85, 082002
Abadie J. et al., 2012b, Phys. Rev. D, 85, 102004
Abramovici A. et al., 1992, Science, 256, 325A
Accadia T. et al., 2012, Virgo Document VIR-0128A-12, available at: https://tds.ego-gw.it/ql/?c=8940
Acernese F. et al., 2009, Virgo Technical Report VIR-0027A-09, available at: https://tds.ego-gw. it/ql/?c=6589
Belczynski K., Kalogera V., Bulik T., 2002, ApJ, 572, 407
Belczynski K., Sadowski S., Rasio F. A., Bulik T., 2006, ApJ, 650, 303
Belczynski K., Taam R. E., Kalogera V., Rasio F. A., Bulik T., 2007, ApJ, 662, 504
Belczynski K., Dominik M., Bulik T., O'Shaughnessy R., Fryer C., Holz D. E., 2010a, ApJ, 715, L318
Belczynski K., Bulik T., Fryer C. L., Ruiter A., Valsecchi F., Vink J. S., Hurley J. R., 2010b, ApJ, 714, 1217
Brown D. A., Zimmerman P. J., 2010, Phys. Rev. D 81, 2, 4007
Coward D. M. et al., 2012, MNRAS, 425, 2668
Carpenter J. M., 2000, AJ, 120, 3139
Clausen D., Sigurdsson S., Chernoff D. F., 2013, MNRAS, 428, 3618
Davis P. J., Kolb U., Knigge C., 2012, MNRAS, 419, 287
Dewi J. D. M., Podsiadlowski Ph., Sena A., 2006, MNRAS, 368, 1742
Dominik M., Belczynski K., Fryer C., Holz D. E., Berti E., Bulik T., Mandel I., O'Shaughnessy R., 2012, ApJ, 759, 52
Dominik M., Belczynski K., Fryer C., Holz D. E., Berti E., Bulik T., Mandel I., O'Shaughnessy R., 2013, ApJ, 779, 72
Downing J. M. B., Benacquista M. J., Giersz M., Spurzem R., 2010, MNRAS, 407, 1946
Downing J. M., Benacquista M. J., Giersz M., Spurzem R., 2011, MNRAS, 416, 133
Duquennoy A., Mayor M., 1991, A&A, 248, 485
Fryer C. L., 1999, ApJ, 522, 413
Fryer C. L., Kalogera V., 2001, ApJ, 554, 548
Fryer C. L., Belczynski K., Wiktorowicz G., Dominik M., Kalogera V., Holz D. E., 2012, ApJ, 749, 91
Gaburov E., Harfst S., Portegies Zwart S., 2009, New Astron., 14, 630
Gieles M., Portegies Zwart S. F., 2011, MNRAS, 410, L6
Goddard Q. E., Bastian N., Kennicutt R. C., 2010, MNRAS, 405, 857
Harris W. E., 1996, AJ, 112, 1487
Harry G. M. (The LIGO Scientific Collaboration), 2010, Class Quantum Gravity, 27, 084006
Hartman J. W., 1997, A&A, 322, 127
Heggie D. C., 1975, MNRAS, 173, 729
Hills J. G., 1989, AJ, 97, 222

Hills J. G., 1992, AJ, 103, 1955
Hopkins A. M., Beacom J. F., 2006, ApJ, 651, 142
Hurley J. R., Pols O. R., Tout C. A., 2000, MNRAS, 315, 543
Kalogera V. et al., 2004, ApJ, 614, L137
Kalogera V., Belczynski K., Kim C., O'Shaughnessy R., Willems B., 2007, Phys. Rep., 442, 75
King I. R., 1966, AJ, 71, 64
Kraicheva Z. T., Popova E. I., Tutukov A. V., Iungelson L. R., 1978, AZh, 55, 1176
Kroupa P., 2001, MNRAS, 322, 231
Kruijssen J. M. D., Pelupessy F. I., Lamers H. J. G. L. M., Portegies Zwart S. F., Icke V., 2011, MNRAS, 414, 1339
Lada C. J., Lada E. A., 2003, ARA&A, 41, 57
Maggiore M., 2008, Gravitational Waves: Volume 1: Theory and Experiments. Oxford Univ. Press, Oxford
Mapelli M., Bressan A., 2013, MNRAS, 430, 3120
Mapelli M., Colpi M., Zampieri L., 2009, MNRAS, 395, L71
Mapelli M., Ripamonti E., Zampieri L., Colpi M., Bressan A., 2010a, MNRAS, 408, 234
Mapelli M., Huwyler C., Mayer L., Jetzer Ph., Vecchio A., 2010b, ApJ, 719, 987
Mapelli M., Ripamonti E., Vecchio A., Graham A. W., Gualandris A., 2012, A&A, 542, A102
Mapelli M., Zampieri L., Ripamonti E., Bressan A., 2013, MNRAS, 429, 2298 (Paper I)
O'Leary R. M., Rasio F. A., Fregeau J. M., Ivanova N., O'Shaughnessy R., 2006, ApJ, 637, 937
O'Shaughnessy R., Kim C., Kalogera V., Belczynski K., 2008, ApJ, 672, 479
Özel F., Psaltis D., Narayan R., McClintock J. E., 2010, ApJ, 725, 1918
Panter B., Jimenez R., Heavens A. F., Charlot S., 2008, MNRAS, 391, 1117
Peters P. C., 1964, Phys. Rev., 136, 1224
Pfahl E., Podsiadlowski P., Rappaport S., 2005, ApJ, 628, 343
Pilyugin L. S., Vílchez J. M., Contini T., 2004, A&A, 425, 849
Porras A., Christopher M., Allen L., Di Francesco J., Megeath S. T., Myers P. C., 2003, AJ, 126, 1916
Portegies Zwart S. F., 2004, preprint (astro-ph/0406550)
Portegies Zwart S. F., McMillan S. L. W., 2002, ApJ, 576, 899
Portegies Zwart S. F., Verbunt F., 1996, A&A, 309, 179
Portegies Zwart S. F., McMillan S. L. W., Hut P., Makino J., 2001, MNRAS, 321, 199
Portegies Zwart S. F., McMillan S. L. W., Gieles M., 2010, ARA&A, 48, 431
Quinlan G. D., 1996, New Astron., 1, 35
Sadowski A., Belczynski K., Bulik T., Ivanova N., 2008, ApJ, 676, 1162
Samsing J., MacLeod M., Ramirez-Ruiz E., 2014, ApJ, 784, 71-94
Siellez K., Boër M., Gendre B., 2014, MNRAS, 437, 649
Sigurdsson S., Hernquist L., 1993, Nature, 364, 423S
Silva-Villa E., Larsen S. S., 2010, A&A, 516, 10
Spitzer L., Jr, 1969, ApJ, 158, L139
Vink J. S., de Koter A., 2005, A&A, 442, 587
Vink J. S., de Koter A., Lamers H. J. G. L. M., 2001, A&A, 369, 574
Voss R., Tauris T. M., 2003, MNRAS, 342, 1169

APPENDIX A: STABLE VERSUS UNSTABLE DCOBs

As we mentioned in Section 3.1, in our paper a binary system is defined as a bound pair, i.e. the most general possible definition. On the other hand, it is reasonable to expect that a portion of these binaries are extremely loose systems, which remain bound only for one (or few) time-step (see the discussion in Section 3.3). In this appendix, we discuss how our results are influenced by our definition of binary systems. In particular, we will compare the main properties of stable and unstable DCOBs.

STARLAB defines as stable binaries those bound pairs with periastron distance $r_p \leq 2.5\,R_{close}$ (see Portegies Zwart et al. 2001), where R_{close} is defined as

$$R_{close} = r_{vir}\frac{m_1 + m_2}{2\,M_{tot}}. \quad \text{(A1)}$$

Then, unstable binaries are binaries with periastron $r_p > 2.5\,R_{close}$. In the following, we consider stable and unstable binaries separately.

A1 DCOB population

Fig. A1 is the same as Fig. 1, but it has been derived considering stable and unstable binaries separately (in the top and bottom panel, respectively). The inset of Fig. A1 shows the average number of BH–BH, NS–NS and NS–BH per YSC as a function of the metallicity. It is remarkable that BH–BH binaries are at least 10 times more numerous than NS–NS and NS–BH binaries, when considering both the stable binary sample and the unstable binary sample. This shows that dynamics has a strong impact on the population of DCOBs, regardless of the distinction between stable and unstable binaries.

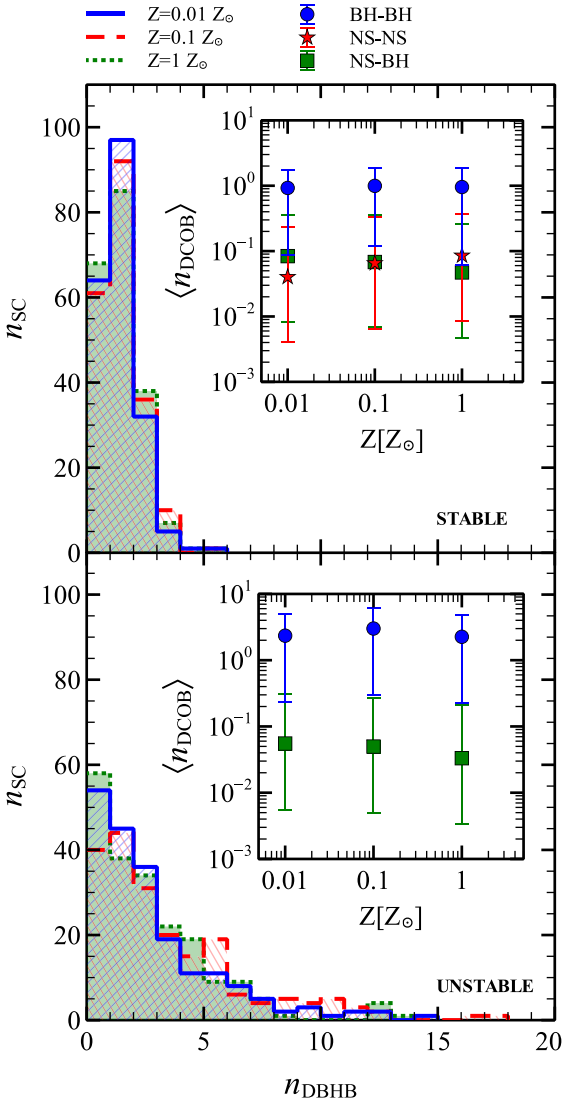

Figure A1. The same as Fig. 1, but we distinguish between stable (top) and unstable (bottom) binaries.

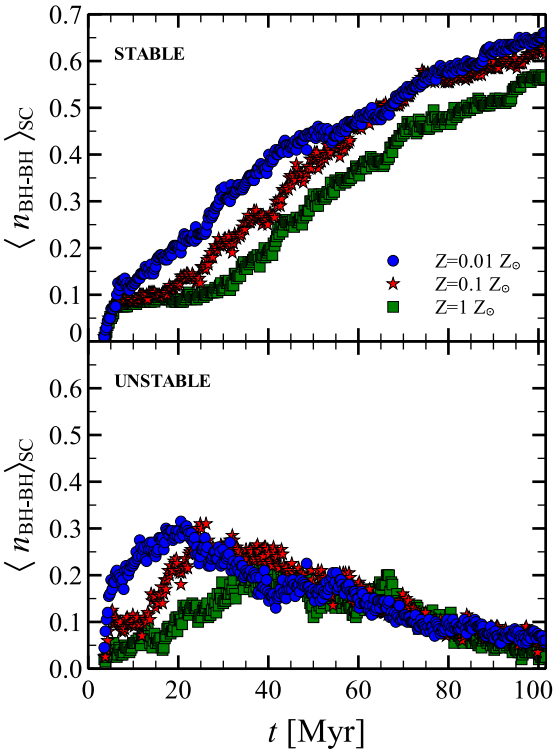

Figure A2. The same as Fig. 2, but we distinguish between stable (top) and unstable (bottom) binaries.

It is also worth noting that we have found no unstable NS– NS binaries. This confirms that only hard (stable) NS–NS binaries can survive (without being disrupted) the two SN explosions of the two progenitors and the dynamical evolution of the binary.

The main panel of Fig. A1 shows the distribution of BH–BH binaries per YSC (integrated over the simulation time). Here, the difference between stable and unstable binaries is quite marked: a single YSC can host up to ∼18 unstable binaries, but only up to ∼6 stable binaries.

Fig. A2 compares the average number of BH–BH binaries per YSC as a function of time for stable (top) and unstable (bottom) binaries. It is worth noting that unstable binaries peak at $10\,\mathrm{Myr} < t < 40\,\mathrm{Myr}$, i.e. immediately after the core collapse: it is reasonable to expect that the formation of loose binaries is triggered by the increase of the central density due to the core-collapse phase (see Mapelli & Bressan 2013). In contrast, the number of stable binaries steadily increases with time (because they tend to survive for a longer time, after their formation). The differences among metallicities that we discussed in Section 3.1 still hold, when considering stable and unstable binaries separately.

A2 Orbital properties and coalescence time-scale

Fig. A3 shows the distribution of semi-major axes of BH–BH, NS–NS and NS–BH binaries at $Z = 0.1\,\mathrm{Z}_{\odot}$, distinguishing between stable (top) and unstable (bottom) binaries. As it is reasonable to expect, most unstable (stable) binaries have semi-major axes $>10^3$ au ($<10^3$ au). However, there are also some unstable binaries with a smaller than that of stable binaries. The reason is that the stability criterion depends not only on the separation of the two objects, but also on their mass (in this sense, it is a hardness criterion) and eccentricity.

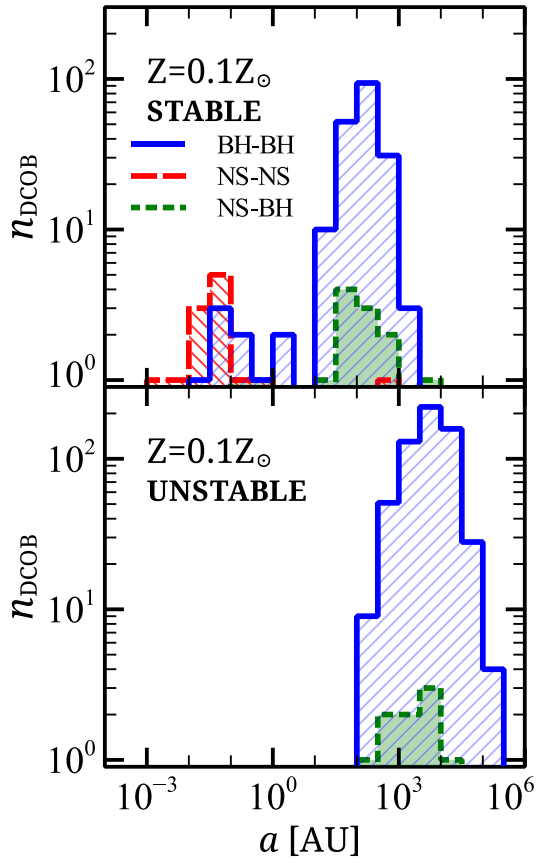

Figure A3. Distribution of semi-major axes a for the stable (top) and unstable (bottom) DCOBs at $Z = 0.1\,\mathrm{Z}_{\odot}$. Lines and colours are the same as in Fig. 5.

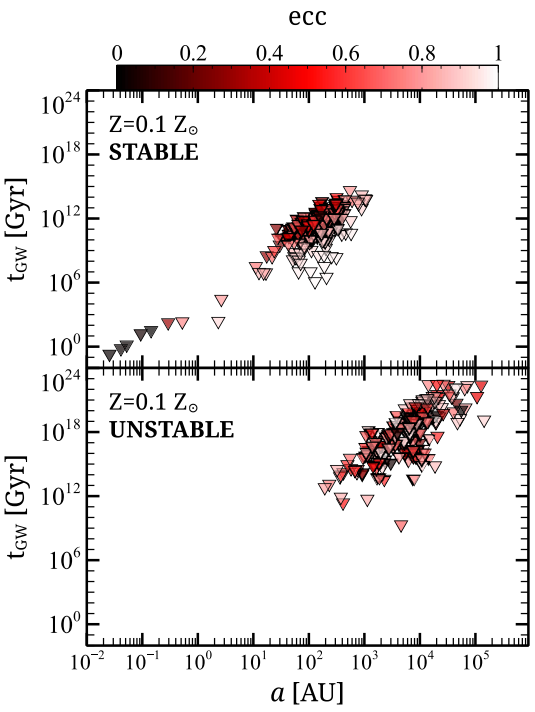

Figure A4. Coalescence time-scale as a function of the semi-major axis for stable (top) and unstable (bottom) BH–BH binaries at $Z = 0.1\,\mathrm{Z}_{\odot}$. Symbols and colours are the same as in Fig. 7.

In the bottom panel of Fig. A3, the most loose unstable binaries have semi-major axes as large as 10^6 au, that is, $\sim$5 pc (similar to the initial YSC tidal radius), with periods comparable to the initial central two-body relaxation time ($\sim$10 Myr, see also Fig. 5). These extremely loose bound pairs are very short lived: it is reasonable to expect that they would completely disappear, if a galactic tidal field would be included in our simulations. On the other hand, these highly unstable systems are completely negligible from the point of view of GW sources.

Fig. A4 confirms that unstable DCOBs are completely negligible from the point of view of GW emission: their coalescence time-scale is by orders of magnitude longer than the Hubble time. Thus, it is sufficient to consider stable binaries alone, when we are interested in possible GW sources.

Finally, in this section, we have considered only YSCs with $Z = 0.1\,Z_{\odot}$ as an example. The same conclusions can be drawn for the other metallicities.

This paper has been typeset from a TEX/LATEX file prepared by the author.